Kırıkcı, F. M., Kahveci, H., Akyazı, Ö. (2024). Enhanced Area Defense: Magnetic Launcher and Sensor Integration. *The Black Sea Journal of Sciences*, 14(2), 760-788.

The Black Sea Journal of Sciences, 14(2), 760-788 2024. DOI: 10.31466/kfbd.1436269

KFBD

Karadeniz Fen Bilimleri Dergisi
The Black Sea Journal of Sciences
ISSN (Online): 2564-7377 https://dergipark.org.tr/tr/pub/kfbd

Araştırma Makalesi / Research Article

Enhanced Area Defense: Magnetic Launcher and Sensor Integration

Furkan Muhammed KIRIKCI[1*], Hakan KAHVECİ[2], Ömür AKYAZI[3]

Abstract

In this article, the most appropriate design method for a field defense system that operates with magnetic field laws by taking audio and video signals as reference is described. The study is important because it eliminates the operator (soldier) factor in the battlefield. Taking into account the effect of capacitor voltage, capacitance value and accelerator winding inductance value, the main criteria for determining the power supply and armature structure of the electromagnetic launcher are proposed. This proposal is made with MATLAB/Simulink software based mathematical model and the differences are explained by comparing with ANSYS Maxwell simulation. The simulated results show that the speed difference between the models is 7%. Additionally, the design methods of the audio and video-based positioning systems that control the system are explained in the study. In this system where signal receiving microphones are positioned in triangular form, a linear algorithm using the time difference method is utilized. By comparing the theoretical mathematical model with the experimental simulation model, the accuracy of the method and the method function is proved. In this study, a deep learning-based target detection system that operates with the YOLO v2 algorithm is used to increase the system's mission execution capacity. The operator is eliminated by switching the system with the signal received from the positioning systems.

Keywords: Electromagnetic launcher system, Acoustic positioning system, Area defense system, Coil gun, ANSYS maxwell analysis.

Güçlendirilmiş Alan Savunması: Manyetik Fırlatıcı ve Sensör Entegrasyonu

Öz

Bu makalede ses ve görüntü sinyallerini referans alarak manyetik alan kanunları ile çalışan alan savunma sistemi için en uygun tasarım yöntemi anlatılmaktadır. Yapılan çalışma sahadaki operatör (asker) faktörünü kaldırdığından dolayı önem arz etmektedir. Kondansatör gerilimi ve sığa değeri ile ivmelendirici sargı endüktans değerinin etkisi dikkate alınarak, elektromanyetik fırlatıcının güç kaynağı ve armatür yapısını belirlemek için temel kriterler önerilmiştir. Bu önerme MATLAB / Simulink yazılım tabanlı matematiksel model ile yapılmış olup, ANSYS Maxwell benzetimi ile karşılaştırılarak oluşan farklılıklar açıklanmıştır. Benzetim sonuçları, modeller arasındaki hız farkının %7 olduğunu göstermektedir. Ayrıca çalışmada sistemin kontrolünü sağlayan ses ve görüntü tabanlı konumlandırma sistemlerinin tasarım yöntemleri anlatılmaktadır. Sinyal alıcı mikrofonların üçgensel formda konumlandırıldığı bu sistemde zaman farkı yöntemini kullanan lineer algoritma kullanılmıştır. Oluşturulan teorik matematiksel model ile deneysel benzetim modeli karşılaştırılarak kullanılan yöntem ve aracı olan fonksiyonun doğruluğu ispatlanmaktadır. Çalışmada sistemin görev gerçekleştirme kapasitesini artırmak için derin öğrenme tabanlı YOLO v2 algoritması ile çalışan hedef tespit sistemi kullanılmaktadır. Konumlandırma sistemlerinden alınan sinyal ile sistem üzerinde anahtarlama yapılarak operatör faktörü aradan çıkarılmaktadır.

Anahtar Kelimeler: Elektromanyetik fırlatıcı sistem, Akustik konumlandırma sistemi, Alan savunma sistemi, Bobin silahı, ANSYS maxwell analiz.

[1,2]Karadeniz Technical University, Department of Electrical and Electronics Engineering, Trabzon, Türkiye, mfurkankirikci@ktu.edu.tr hknkahveci@ktu.edu.tr
[3] Karadeniz Technical University, Department of Energy Systems Engineering, Trabzon, Türkiye, oakyazi@ktu.edu.tr

[*]Sorumlu Yazar/Corresponding Author
Geliş/Received: 13.02.2024 **Kabul/Accepted:** 29.05.2024 **Yayın/Published:** 18.06.2024

1. Introduction

Since the first war in the history of the world, systems of warfare have evolved from muscle power to chemical interaction, and today have reached a new stage of evolution with electrical interaction. The electromagnetic launcher systems that emerged in this stage of evolution throw low or high mass objects with electromagnetic force, independent of chemical reactions in the sectors of defense and transportation. This evolution is changing the paradigms of warfare and transportation technologies, offering more efficient, quiet, reliable, economical and sustainable solutions.

Electromagnetic launcher systems have potential use in the defense industry and have a structure without electrical and physical contact between the pulse power module and the armature circuit (Baharvand et al., 2021). Electrification of weapons minimizes recoil force and explosion signs of the projectile, while enhancing the initial speed of the projectile and making ammunition storage and transportation processes more advantageous due to the absence of gunpowder (Praneeth et al., 2022). The historical origin of the coil gun, which is the focus of this study, begins with the "SIVA" gun developed by Benningfield in the United States in 1844 (McNab, 1999). Theoretically, the fact that there is no limit to the speed of movement of the electromagnetic field means that there is no speed limit for the accelerated object. This makes electromagnetic launcher systems interesting and capable of being developed. The circuit of the winding type electromagnetic launcher is given in Figure 1.

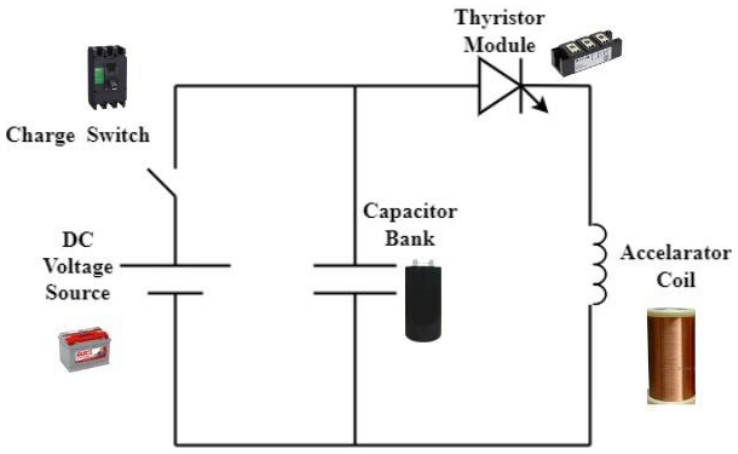

Figure 1. Winding Type Electromagnetic Launcher Model

Since there is high current or voltage in electromagnetic launcher systems, thyristors are preferred in semiconductor switch selection (Akyazı et al., 2015). In the circuit in Figure 1, when the thyristor is in cut-off mode, the charge switch is turned off at t = 0 and the charge is stored in the capacitor bank with the voltage change according to equation 1. The C value in the equation is the capacitance value of the capacitor as "Farad".

$$i_C = C.\frac{dV_c}{d_t} \quad (1)$$

After t = 0, the thyristor is switched to conduction mode by using a current triggered signal. This signal is generated by the visual (image) and acoustic (sound) detection systems within the area defense system. When the thyristor switches to conduction mode, a high current change occurs on the accelerator winding in a short time according to equation 2. Here L is the inductance value of the coil as "Henry". The amount of energy stored in parallel connected capacitor groups at t = 0 is given in equation 3.

$$V_L = L.\frac{di_L}{d_t} \quad (2)$$

$$E_C = \frac{1}{2}.C.V^2 \quad (3)$$

When equations 1, 2 and 3 are analyzed, it is seen that the voltage applied to the capacitor bank and the capacitance value must be high in order for an electromagnetic launcher system with an accelerator winding to fire at high speeds. In addition, it is important that the damping process on the coil is completed as quickly as possible. The main purpose of these systems is to achieve high current changes on the coil.

Thanks to the current change occurring on the cylinder wound coil, a magnetic field whose amplitude changes over time is obtained. The projectile in the cylinder, which has a high magnetic permeability, moves by following the point where the field is strongest. As the projectile moves, the reluctance of the system will change until it reaches a minimum reluctance value (for a given flux level) when the center of the projectile intersects the center of the coil (Bresie, 1991).

The electromagnetic launcher system in Figure 1 is considered as a simple RLC circuit. Therefore, although the launch speed is theoretically infinite, there are limiting factors. In order to efficiently convert the electrical charge into a magnetic field, the RLC circuit parameters must be accurately calculated. In addition, the triggering time needs to be set to half a period due to the reverse force acting on the projectile after the midpoint of the winding (Wang et al., 2016). Since the performance of electromagnetic launcher systems is directly proportional to the current damped on the coil element, the resonant state should be taken as the lowest value of the system reactance.

The current damped on the coil must be in only one direction, otherwise the acceleration of the projectile may decrease or the launch may not be realized due to the reverse force applied by the coil. Therefore, critical damping must occur on the RLC circuit (Kırıkcı, 2023).

The parameters to be considered in the design of the electromagnetic launcher according to the resonance state are the damping period in equation 4, the damping resistance in equation 5 and the energy consumed on the coil due to damping in equation 6 (Akyazı, 2006). The peak value of the damping current in equations 2 and 6 is given in equation 7.

$$T = \pi.\sqrt{L.C} \tag{4}$$

$$R^2 = \frac{4L}{C} \tag{5}$$

$$E_L = \frac{1}{2}.L.i^2 \tag{6}$$

$$I_{max} = \frac{V_0}{e}.\sqrt{\frac{C}{L}} \tag{7}$$

In the analysis of electromagnetic launcher systems, the magnetic circuit must be taken into account as well as the electrical circuit. The magnitude and direction of the magnetic field and the size of the projectile to be used affect the value of the electromagnetic force. In addition, in a paper in the literature (Sari, 2023), a proposal is presented to increase the system efficiency by modifying the projectile starting position and size. In another study (Su et al., 2021), the effect of coil positions and distance between coils on the system efficiency of a launcher with multiple accelerator coils arranged in series is evaluated. At the same time, the inductance value of the accelerator winding should be designed in accordance with the system geometry and current parameters (Fan et al., 2020).

Reluctance accelerators have been documented as relatively inefficient devices with efficiencies of ~2% for optimized systems (Slade, 2005). Although there is no theoretical speed limit, system efficiency has remained at low reference values in the literature. This study was done to determine the optimal design suggestions for an electromagnetic launcher system in an area defense system. For the design suggestions, mathematical models in the literature were reviewed and our own model was created in MATLAB / Simulink simulation environment. However, in order to determine the accuracy of this model, a comparison was made with the same parameters in ANSYS Electronics simulation environment including Maxwell' s laws.

As a result of the chemical reaction in firearms, high intensity sound and shock waves are generated in the barrel. Acoustic-based positioning systems are mission mechanisms that receive sound and shock waves and perform target detection using signal processing methods. The system is usually used by placing at least four sensitive microphones in a predetermined geometry, camouflaged and protected. Studies on acoustic positioning in Türkiye have only recently started

(Özuğur et al., 2016). Today, considering the geographical location of our country, it is of great importance to protect borders, outposts and military areas and to provide tactical strategy superiority with these systems.

When the system is designed on a product basis, if it is to be positioned at long distances on the coordinate axis, axial positioning according to the center must be done very well. For all these calculations to be done correctly, the structure of the sound, the characteristics of the microphones to be used, the mathematical model, the signal processing technique, the arrival difference method and the position determination issues must be considered effectively. In this study, the mathematical model of the system together with the defense system is presented.

YOLO (You Only Look Once) algorithm was used for image analysis in the area defense system. YOLO is fast because it performs object detection in a single analysis. This algorithm divides the image into bounding boxes, analyzes the presence of objects within these boxes and increases the accuracy rate by using confidence scores. The Non-Maximum Suppression algorithm selects bounding boxes with high confidence scores and includes them in the dataset. This method provides an effective object detection by increasing the accuracy rate (Jiang et al., 2022).

In this study, a model of a field defense system operating with magnetic field laws is designed in which a projectile is fired by switching method with reference to audio and video signals. The proposed design criteria for the accelerator wound coil weapon can play a key role in determining the power supply and armature structure of these systems. This focus on the design of electromagnetic launcher systems aims to minimize the impact of the operator factor by increasing system efficiency.

In the literature section, studies on electromagnetic launcher systems are tabulated in chronological order. The table also indicates the parameter changes made to increase the efficiency of the launcher systems. In the materials and methods section, mathematical expressions of the models designed in MATLAB and ANSYS simulation environments and comparison scenarios are given. In the findings section, the results obtained according to the comparison scenarios are shared on the same graph. In the results section, the design criteria are shared in bulleted form.

2. Literature Survey

The first scientific study in history was done by Dr. Charles G. Pages in Washington, D.C. in 1845 (Pages, 1845). Later, "Birkeland’ s Electromagnetic Gun: A Historical Review" by Kristian Birkeland in Norway in the early 1900s is an important milestone in the literature (Egeland, 1989).

During World War I, in 1916, Fauchon-Villeplee’ s work was published in book form (Fauchon, 1920). This source describes the principles of the DA rail-type electromagnetic launcher.

Engel and his colleagues designed a rifle-caliber and barrel-type electromagnetic launcher in 2001. They obtained 15 kA at the barrel with a charging voltage of 450 V and measured the speed of a 1-gram projectile weighing 450 m/s leaving the rails (Engel et al., 2001). In Table 1, examples of parameter modification studies on the current mathematical model of electromagnetic launcher systems are given chronologically.

Table 1. Studies in the Literature

Reference	Year	Product Type	Design Criteria	Speed (m/s)
(Ege et all.)	2016	Wrapped	Coil Trigger Time	1,75
(Wang et all.)	2016	Wrapped	Coil Trigger Time	32,4
(Dong et all.)	2018	Series Wrapped	Number of Armatures - Capacitor Parameters	814
(Fan et all.)	2020	Wrapped	Energy Impact Method - Armature Structure	360
(Liang et all.)	2021	Wrapped	Damping Resistance	27.4
(Lu et all.)	2022	Wrapped	Simulation Model	7 - 8
(Zhao et all.)	2023	Wrapped	Improved Power Supply	19.8
(Wan et all.)	2023	Rail	Cooling Type	-
(Abdo et all.)	2023	Wrapped	Reluctance-Charge Voltage	14.9

3. Materials and Methods

In this section, the design of the model with parameter changes and the two models that provide switching will be explained. Three different simulation programs MATLAB / Simulink, Audacity and ANSYS Electronics Maxwell were used in the design phase of the model. The main schematic of the designed model is presented in Figure 2 and the flowchart showing the operation of the system is shown in Figure 3. The power stage, voltage gain stage, firing stage and measurement block of the system were simulated in MATLAB / Simulink software environment. In addition, the human detection and acoustic positioning system is modeled in MATLAB / m-file simulation environment. In the last scenario, a design was created on ANSYS Maxwell to determine the model accuracy.

According to the flowchart in Figure 3, the system first performs human detection with the target detection algorithm. In case of human detection, the system (charge) switch on the system is activated and the voltage value of the capacitors in the load bank is adjusted to the voltage value determined at the converter output. When sound signals are detected in the acoustic positioning system, a shot is fired.

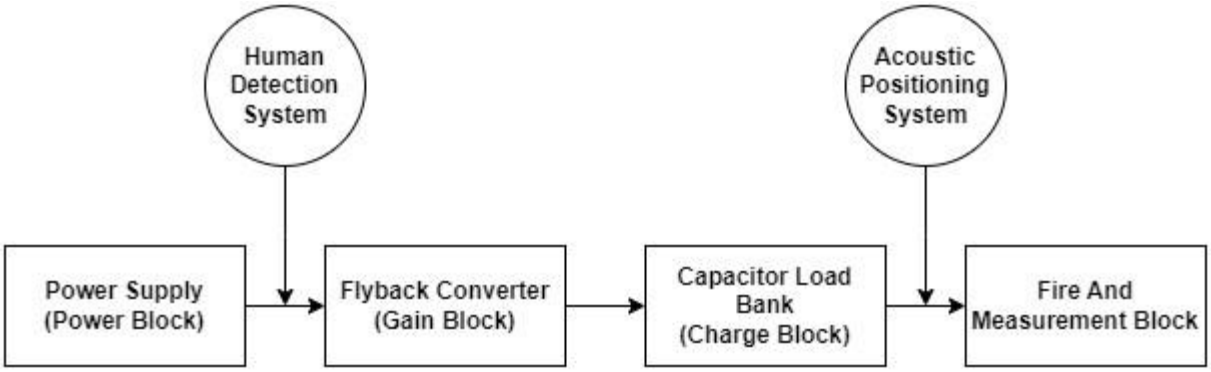

Figure 2. Electromagnetic Launcher System Model

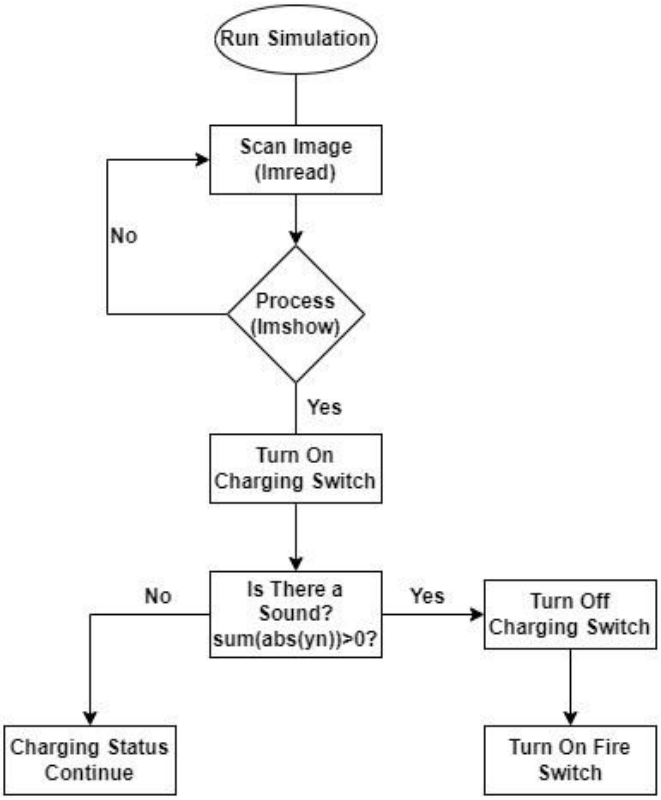

Figure 3. Electromagnetic Launcher System Model Operation Plan

3.1. Electromagnetic Launcher System Simulation Model

In this section, the system modeled in MATLAB / Simulink simulation environment to determine the parameters affecting the performance of electromagnetic launcher systems is given in Figure 4. The system consists of a DC voltage source, a flyback converter that provides voltage gain, a firing model that performs the acceleration task, in addition to target and asset detection systems that generate switching signals.

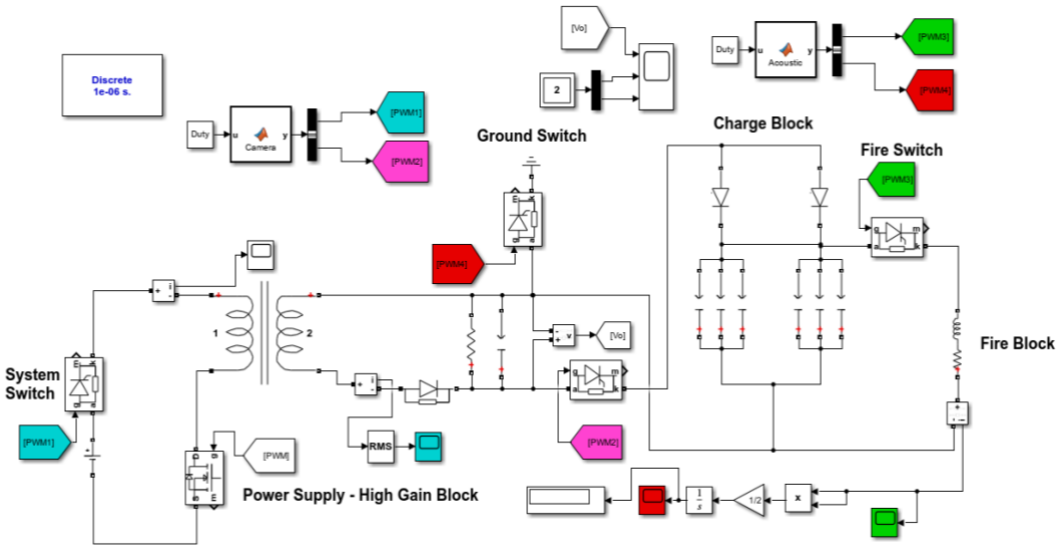

Figure 4. Electromagnetic Launcher System Simulink Simulation Model

3.1.1. Flyback Charge Circuit Model

In electromagnetic launcher systems, there are two independent cycles, charge and discharge. Voltage gain directly affects the system performance and can be achieved by different methods. Generally, voltage adjustment is possible using power supplies fed from AC sources; however, the requirement for the launcher systems to be portable may reduce the possibility of the system to perform the mission. For this reason, it is thought that the use of direct current (DC) sources may be more appropriate in electromagnetic launchers with destructive tasks.

Due to the design difficulties of the DC-DC boost converter and the power losses that occur in flyback converter, it is not considered suitable for this field. It can be realized with a classical Flyback converter, which is a low-cost and reliable system with no electrical connection between input and output. The general circuit topology of a Flyback converter is presented in Figure 5.

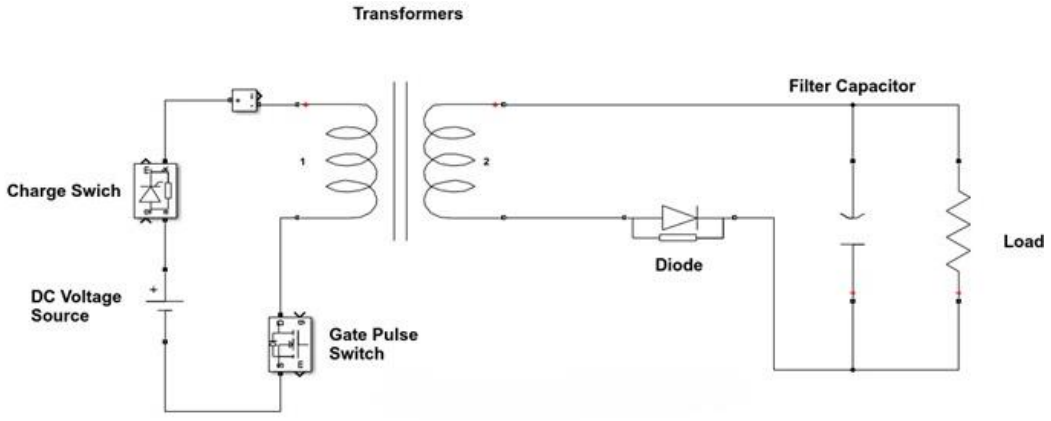

Figure 5. Flyback Converter General Circuit Topology

Flyback converters have continuous current and discontinuous current modes depending on the value of the magnetic field energy of the transformer. In continuous current mode, the current on the inductance and therefore the magnetic field never goes to zero. In order not to stop the charging current of the capacitors on the system, continuous current operation mode is preferred and the parameters are set according to this mode.

In the conduction mode of the MOSFET in the converter, the DC source is connected to the primary terminals of the transformer and the input voltage and the primary voltage are equal to each other. The relation in equation 2 gives the value of the voltage induced in the transformer in the flyback converter. The relation of the unit time changes in equation 2 is given in equation 8. D in the equation gives the fill rate of the gate signal applied to the MOSFET and T gives the switching period.

$$\Delta t = D.T \tag{8}$$

Using the relations in equations 2 and 8, the relation of the current change on the coupling element is given in Equation 9.

$$\Delta i_L = \frac{V_1.D.T}{L} \tag{9}$$

It is seen in the literature that the current ripple on the transformer with coupling element is accepted as 40% of the coil current in continuous current operation mode. If the inductance value (L) of the transformer with coupling element is calculated from equation 9, equation 10 is obtained. Here f is the switching frequency value of the MOSFET.

$$L = \frac{V_1.D}{\Delta i_L.f} \tag{10}$$

It is very important to determine the correct winding ratio of the coupled transformer in the converter. The ideal ratio is determined from equation 11 to provide the desired voltage gain at high switching frequency and to avoid long-time high current draw on the transformer. N2 and N1 symbolize the number of turns of the transformer.

$$\frac{N_2}{N_1} = \frac{V_{out}}{V_{in}}.\frac{(1-D)}{D} \tag{11}$$

If the MOSFET operates in conduction mode, the output load will be fed by the load stored in the capacitance. Therefore, when determining the capacitance value in the design, it should be selected large within the appropriate values. Another consideration when determining the capacitance

value is the voltage ripple factor. Depending on the voltage ripple value during the design phase, the capacitance (C) value is determined from equation 12. The parameter selection of the field defense system with detailed parameter equations is obtained from the relevant relation (Kırıkcı, 2023).

$$\frac{\Delta V_{out}}{V_{out}} = \frac{D}{R.C.f} \tag{12}$$

The converter parameters of the scenarios considered in this paper are presented in detail in Table 2.

Table 2. Flyback Converter Parameters

Flyback Converter Circuit Parameters		
	Situation (1)	Situation (2)
Input Voltage (Volt)	24	24
Output Voltage (Volt)	140-150	235-250
Capacitance (Farad)	$4.5x10^{-4}$	$4.3x10^{-4}$
Resistance (Ohm)	200	335
Inductance (Henry)	$4.965x10^{-3}$	$2.757x10^{-3}$
Inductance Ampere (Amper)	7.25 - 7.5	12.5
Power (Watt)	98-113	172-187
Turns Ratio (N_1/N_2)	4	7
Switch Voltage Value (V_{DS})	65	65

3.1.2. Fire Circuit Model

It is the model that performs the firing process by damping the energy stored at the terminals of the load bank on the coil. The parameters of the firing model were calculated based on equations (1-7). During the setting up of the firing scenarios, the damping resistance value given in equation 5 plays a critical role in determining the parameters. The inductance value of the accelerator winding in the firing model is derived from equations 4, 5 and 7. In order to interpret the order of determination of the parameters and their effect, firing scenarios were created on the system.

In these scenarios, the capacitor voltage, capacitance value and the inductance value of the accelerator winding will be changed respectively. Additionally, the firing in the last scenario will be performed in two different simulation programs in order to comment on the speed calculations based on the mathematical model in the literature. The parameter data of the scenarios are given in tables 3, 4, 5 and 6.

Table 3. First Scenario Fire Model Parameters

Scenario (1)		
Parameters	Situation (1)	Situation (2)
Capacitance Voltage (Volt)	145	238
Capacitance (Farad)	$150x10^{-3}$	$150x10^{-3}$
Resistance (Ohm)	$45x10^{-3}$	$45x10^{-3}$
Inductance (Henry)	$75x10^{-6}$	$75x10^{-6}$
Firing Period (ms)	11	11

Table 4. Second Scenario Fire Model Parameters

Scenario (2)		
Parameters	Situation (1)	Situation (2)
Capacitance Voltage (Volt)	145	85
Capacitance (Farad)	$150x10^{-3}$	$1500x10^{-3}$
Resistance (Ohm)	$45x10^{-3}$	$14.1x10^{-3}$
Inductance (Henry)	$75x10^{-6}$	$75x10^{-6}$
Firing Period (ms)	11	33

Table 5. Third Scenario Fire Model Parameters

Scenario (3)		
Parameters	Situation (1)	Situation (2)
Capacitance Voltage (Volt)	145	145
Capacitance (Farad)	$150x10^{-3}$	$150x10^{-3}$
Resistance (Ohm)	$45x10^{-3}$	$141x10^{-3}$
Inductance (Henry)	$75x10^{-6}$	$750x10^{-6}$
Firing Period (ms)	11	33

Table 6. Fourth Scenario Fire Model Parameters

Scenario (4)		
Parameters	Situation (1)	Situation (2)
Capacitance Voltage (Volt)	5000	5000
Capacitance (Farad)	$1.2x10^{-3}$	$1.2\ x10^{-3}$
Resistance (Ohm)	0.2	0.2
Inductance (Henry)	$12\ x10^{-6}$	$12\ x10^{-6}$
Firing Period (ms)	0.75	0.75

3.1.3. Acoustic Positioning System Model

This model uses a time-differential linear algorithm for location detection based on the presence of sound. Various combinations of microphones in various geometric shapes can be placed around a

reference microphone to detect the sound signal (Cakir et al., 2012). There are three microphones placed in a triangular position in a circle around the reference microphone. As these microphones are positioned at oblique angles relative to the reference microphone, they must be positioned using a carefully designed stabilization system. Millimetric errors can degrade the position accuracy at large distances from the reference coordinate axis. Furthermore, considering the cost of the system, increasing the number of condenser microphones with wide dispersion can have a negative impact on cost. Therefore, it is important to keep the number of microphones to be used in the system to a minimum and to choose the right geometry. Figure 6 shows the geometrical plan of the system.

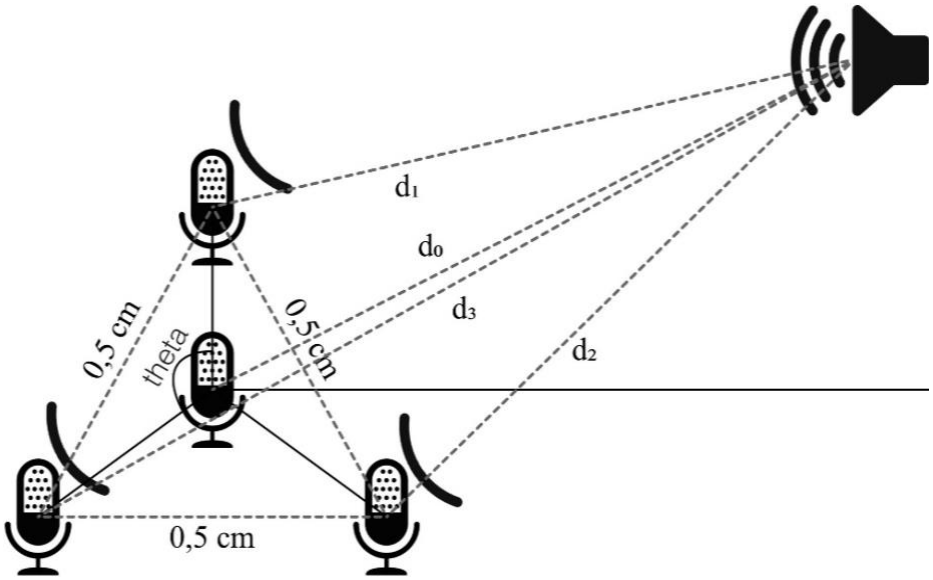

Figure 6. Acoustic Positioning System Model

In order to model the acoustic positioning system experimentally in the mfile simulation program, the mathematical model of the system should be created with geometric calculations in the theoretical part and the experimental part should be started by creating sound recordings with these calculated parameters. Figure 7 shows the flowchart for the theoretical part. In this section, the distance of the audio signals to be created in Audacity from the microphones is calculated. For this, the target is assumed to be predetermined.

In the acoustic positioning system created in Figure 6, the attack is assumed to come from the 1st region (northeast). There is one reference microphone at the center point of the coordinate axis and three microphones in a triangular position. The distances between the microphones and the sound are symbolized as d(n). The positions of the microphones are found from equations 13, 14 and 15.

$$\theta = \frac{360}{M_{microfone} - 1} \tag{13}$$

$$\beta = \frac{180 - \theta}{2} \tag{14}$$

$$r_{real} = \frac{a}{2 \,.\cos^{-1}(\beta)} \tag{15}$$

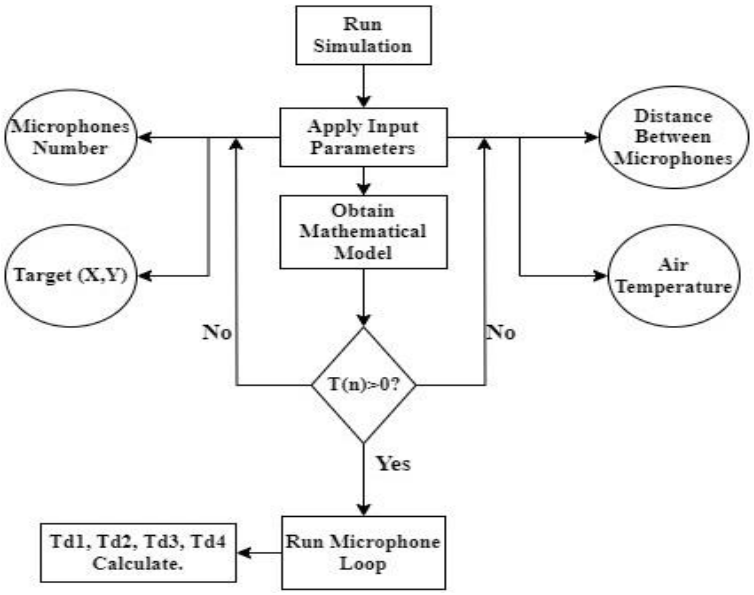

Figure 7. Acoustic Positioning System Theoretical Flowchart

θ symbolizes the dispersion angle of the microphones, a symbolizes the distance between microphones and β symbolizes the angle of the microphones with the coordinate axes as shown in Figure 6. The real radius is the radius of the circle in which the microphones are positioned, that is the distance between the reference microphone and the microphones. In Equations 16, 17 and 18, the distance of the microphones to the sound source, the distance difference to the reference microphone and the time difference are given, respectively.

$$\mathrm{d(n)} = \sqrt{\left(x_{sound} - x_{microfone}\right)^2 + (y_{sound} - y_{microfone})^2} \tag{16}$$

$$\mathrm{T(n)} = \mathrm{d(reference)} - \mathrm{d(n+1)} \tag{17}$$

$$t_{difference} = \frac{T(n)}{Sound\ Speed} \tag{18}$$

After the time difference between the microphones is found in equation 18, the time difference between the audio signals is created in the Audacity program (Kırıkcı, 2023). After the audio signal

files are created, the experimental flow diagram of the acoustic positioning system given in Figure 8 can be applied.

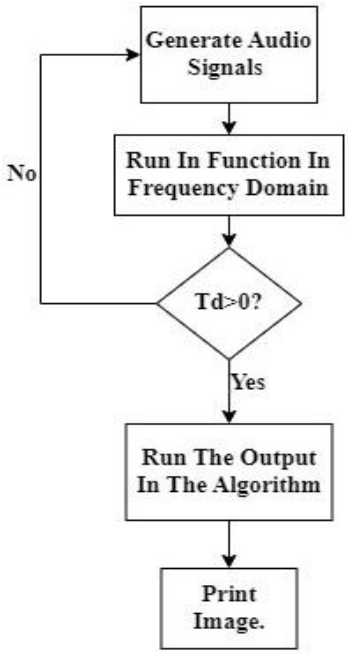

Figure 8. Acoustic Positioning System Experimental Flowchart

As a result of the chemical reaction, two signals, sound and shock waves, are generated in the barrel. Shock waves are more accurate in determining the projectile direction that is, the angle of the projectile, while the muzzle sound is more accurate in determining the target position. Therefore, target detection is easier when both are used (Kaushik et al., 2005).

The algorithm makes calculations based on the sound recordings from the four microphones used in the system. In MATLAB, the sampling value and the intensity value of the sound will be taken from this recording and the signal will be associated with the cross-correlation function (Urruela et al., 2006).

The cross-correlation function is a function that is widely used for signal processing in location detection applications. The fourier transforms of the cross-correlation function are given in equations 19 and 20.

$$R_{12}(\tau) = \int_{-\infty}^{\infty} g_1(\tau).{g_2}^*(\mathrm{t}-\tau).\mathrm{dt} \tag{19}$$

$$R_{21}(\tau) = \int_{-\infty}^{\infty} g_2(\tau).{g_1}^*(\mathrm{t}-\tau).\mathrm{dt} \tag{20}$$

In Equation 19, $g_1(\tau)$ is the Fourier transform of the reference microphone and $g_2{}^*(\mathrm{t}-\tau)$ is the Fourier transform of the delayed sound of the same length. After taking the conjugate of the delayed audio signal and multiplying it by the first audio signal, the inverse Fourier transform of the resulting values are taken and then the values in the frequency domain are converted back to the time domain. During this multiplication process, each sample of the second audio matching the first audio is multiplied individually to determine the position where the maximum amplitude occurs. Therefore, the position that maximizes $R_{12}(\tau)$ indicates the amount of delay for us.

As in the theoretical process, the time differences obtained as a result of the function are multiplied by the speed of sound to calculate the distance differences. In order to determine the target experimentally, these distance differences need to be processed in the algorithm with a time difference method based on geometric calculations. As a result, both theoretical and experimental working methods are applied in the model and the acoustic positioning system is built by establishing a relationship between these two models. The output results of the model will be shared in the findings section. Since the outputs of the designed model are directly transferred to the Simulink simulation interface, switching is done on the system depending on the (y) value indicating the intensity of the sound, which is the result of the cross-correlation function.

3.1.4. Image Processing System Model

In the electromagnetic launcher model, a continuous connection from the power supply to the charging circuit leads to a reduction in the lifetime of the power source. Since a DC source is used, it is important that the source voltage does not drop below 70%. Therefore, switching is required at the input of the system. The system switching will be done with the YOLO (You Only Look Once) algorithm available in MATLAB and image processing technique will be used.

The YOLO v2 object detector was chosen as the analyzer used in MATLAB / Mfile. The image size provided as input to the system must be equal to or larger than the neural input size of the pre-trained detector. The image's pixel height (H), pixel width (W), channel size (C) and number of images in the array (B) parameters need to be optimized.

It has been determined that YOLO performs real-time object detection faster than other algorithms. The main reason for this faster performance is that it can instantly evaluate the class and coordinates of all objects by passing the image through neural networks in a single pass. This process is based on treating object detection as a single regression problem (Jiang et al., 2022).

For human detection, the image presented to the system is first divided into an SxS grid. Each grid determines the presence of a human, its midpoint if it exists, its length and height if it is within

the midpoint, and which class it belongs to. Then, a prediction vector is created for each grid and the error functions for each are evaluated.

In order to classify the image provided as input and obtain the accuracy value, the algorithm needs to be processed on the system. For this process, the "[bboxes, scores]" loop is used in MATLAB (Dalal et al., 2005).

Once the image is suitable for the algorithm, a loop must be created to output the histogram values and process these values. The processing of the image into the algorithm is performed using the "visualization" command. The function "[hog1, visualization]" can be used for object detection based on histogram values.

3.1.5. Speed Measurement Model

The conversion of electrical energy into magnetic energy is realized in the firing model. The potential energy stored in the capacitors is transformed into magnetic energy on the coil. Equations 3 and 6, respectively, express the potential energy relations on the capacitor and the coil. The potential energy, indicated as the initial energy, is transformed into the kinetic energy form in equation 21. Likewise, the projectile speed is obtained by converting the coil energy expressed in equation 6 into the kinetic energy form in equation 21. Using these equations, a speed measurement model was created using MATLAB/Simulink.

$$E_{kinetic} = \frac{1}{2} . \mathrm{m} . v^2 \tag{21}$$

Electromagnetic launcher systems can not transfer all of the initial energy to the projectile as kinetic energy. Losses occur in the system due to electrical losses in the circuit elements in the firing model and leakage fluxes in the winding model. When the relevant studies in the literature are examined, it is observed that the system efficiency is generally between 1% and 5% in low power applications (≤10kW) (Inger, 2023).

4. Findings

In this section, the results of the modeled electromagnetic launcher system in MATLAB / Simulink and ANSYS Maxwell simulation program and the outputs of the target and human detection algorithm will be shared. The system parameters are determined according to Equation (1-20) in the paper. Simulation times were selected depending on the desired parameter changes in the scenarios.

4.1. First Scenario Results

In this scenario, the charging voltage value of the capacitors is increased from 145 Volts to 238 Volts, keeping all parameters constant. An analysis on the effect of the voltage value on the firing theory will be carried out. Due to the low power converter in the power stage, an increase in the charging time is expected if the capacitor charging voltage is increased. Simulation was performed by adapting the charging time required for the capacitors. Figure 9 shows the damped current graph on the coil.

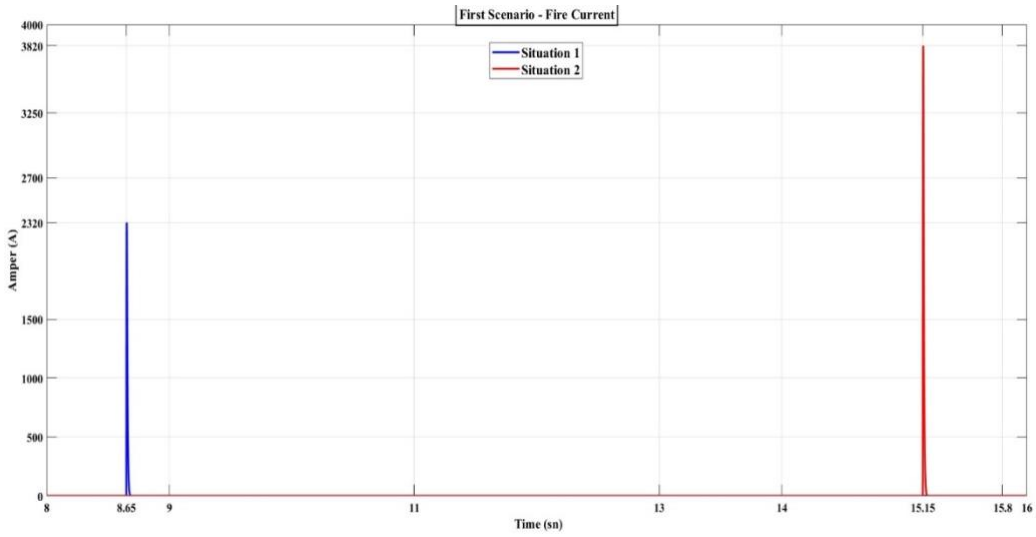

Figure 9. Scenario 1 – Firing Current Graph

When the voltage value of the capacitors increases, the peak value of the current observed on the coil increases from 2320 A to 3820 A. As the peak value of the current damped on the coil increases, according to equation 6, the coil energy is expected to increase and accordingly the speed is expected to increase. Figure 10 shows the charge-discharge curves of the situations and Figure 11 shows the graphs of the projectile speed.

When the voltage value of the load bank is increased from 145 V to 238 V, the potential energy at the capacitor terminals will increase and an increase in the coil energy will be observed. As a result, the projectile speed will increase from 6.345 m/sec to 17.15 m/sec as shown in the graphs. Considering equations 1, 2, 3, 6 and 7, the efficiency comparison between situations 1 and 2 for a 1-gram projectile shows that a voltage increase of 65% at low voltage levels leads to a 2.2% point increase in system efficiency.

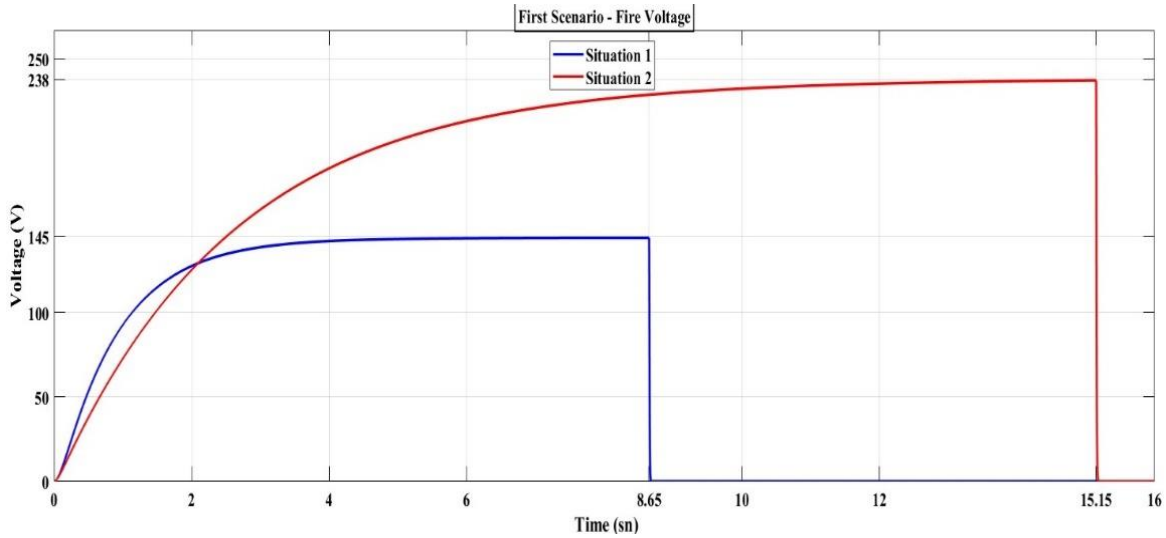

Figure 10. Scenario 1 – Firing Voltage Graph

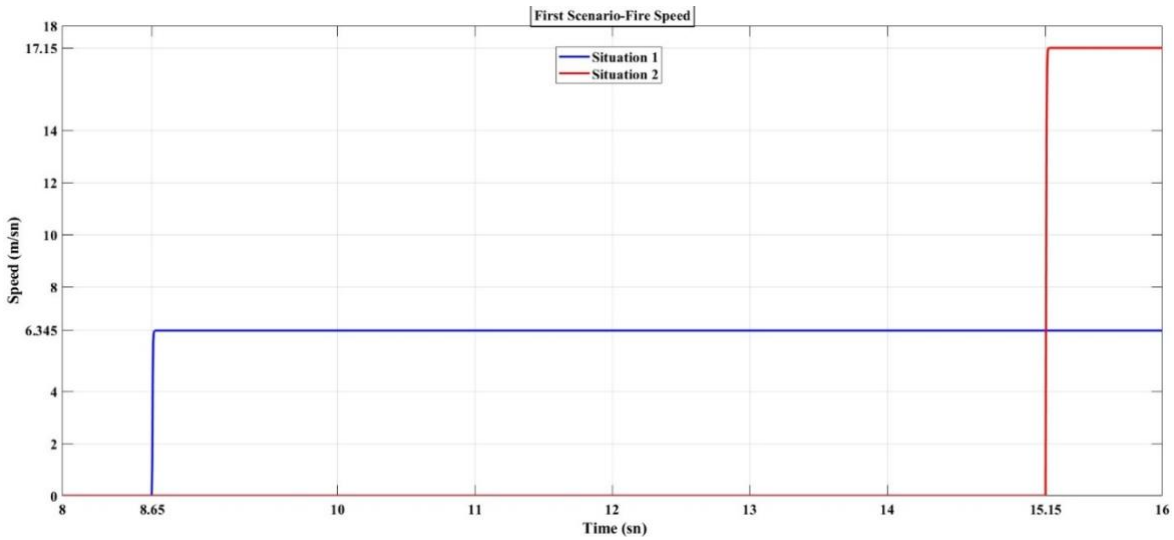

Figure 11. Scenario 1 – Firing Speed Graph

4.2. Second Scenario Results

In this scenario, the equivalent capacitance of the load bank is increased by a factor of 10. Depending on the change of the capacitance value, the damping resistance value in the critical damping state is also selected. Charging time will be kept constant in situation 1 and situation 2. As the capacitance value of the capacitors increases within the constant time, the charging voltage value will decrease. In this scenario, the change in system efficiency depending on the ratio of increase in capacitance value to decrease in voltage value will be analyzed. Figure 12 shows the damped current graph on the coil. Figures 13 and 14 show the capacitor charging voltages and projectile speed values respectively.

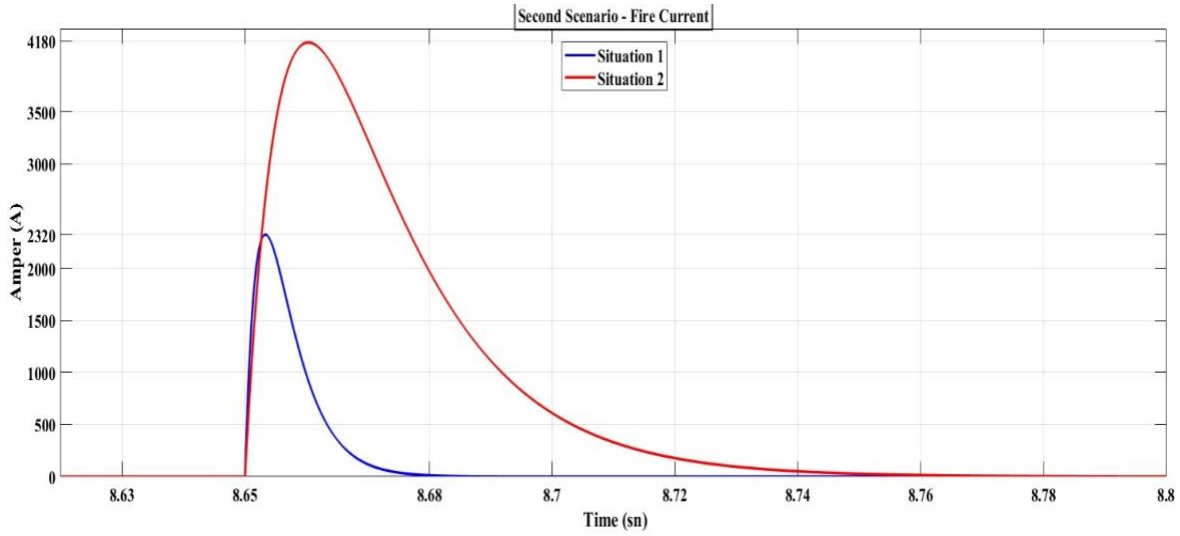

Figure 12. Scenario 2 – Firing Current Graph

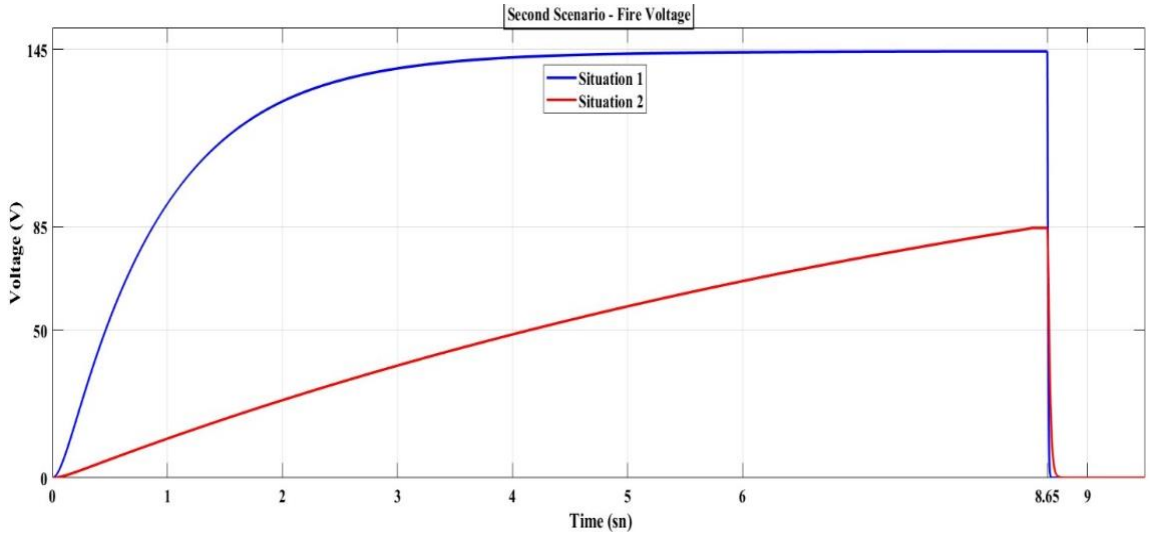

Figure 13. Scenario 2 – Firing Voltage Graph

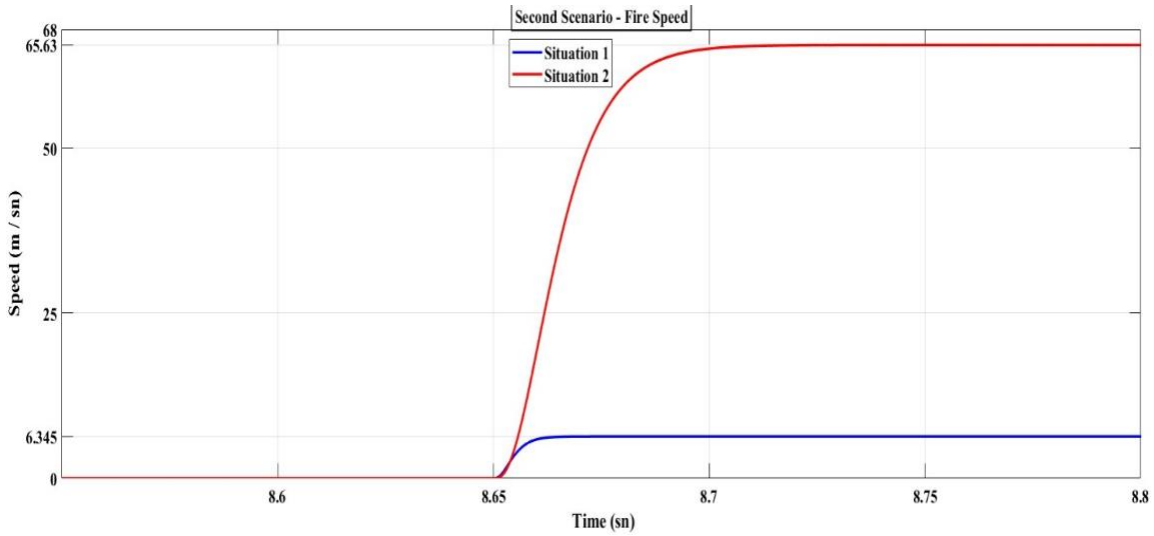

Figure 14. Scenario 2 – Firing Speed Graph

When the voltage value of the capacitors is decreased and the capacitance value is increased, the peak value of the current on the coil increases up to 4180 A. As the peak value of the current damped on the coil increases, according to equation 6, the coil energy is expected to increase and accordingly the speed is expected to increase. Although there is a 40% decrease in the voltage value of the load bank, the potential energy stored at the terminals of the capacitor will increase and an increase in the coil energy will occur. Because, this is a ten-fold increase in the capacitance value increases the energy value in equation 3. As a result, the projectile speed increases to 65.63 m/sec as seen in the graph. Considering equations 1, 2, 3, 6 and 7, in the efficiency comparison between situations 1 and 2 over 1 gram projectile, a 38.5% improvement in system efficiency is observed when a ten-fold increase in capacitance is achieved with a 40% voltage drop.

4.3. Third Scenario Results

In this scenario, the inductance value of the coil in the firing model is increased ten-fold. Depending on the change in the inductance value of the coil, the damping resistance value in the critical damping state was also changed. Figures 15 and 16 show the firing current and firing speed graphs respectively. When the inductance value of the coil is increased, it is observed that the peak value of the current occurring on it decreases up to 747.5 A. As the peak value of the current damped on the coil decreases, according to Equation 6, it is expected that the coil energy decreases and thus the speed decreases. As a result, as shown in Figure 16, a decrease of up to 2.057 m/sec is observed in the speed of the projectile. In the efficiency comparison between situations 1 and 2 over a 1 gram projectile, a 1% decrease in system efficiency is observed when the inductance value is increased ten-fold.

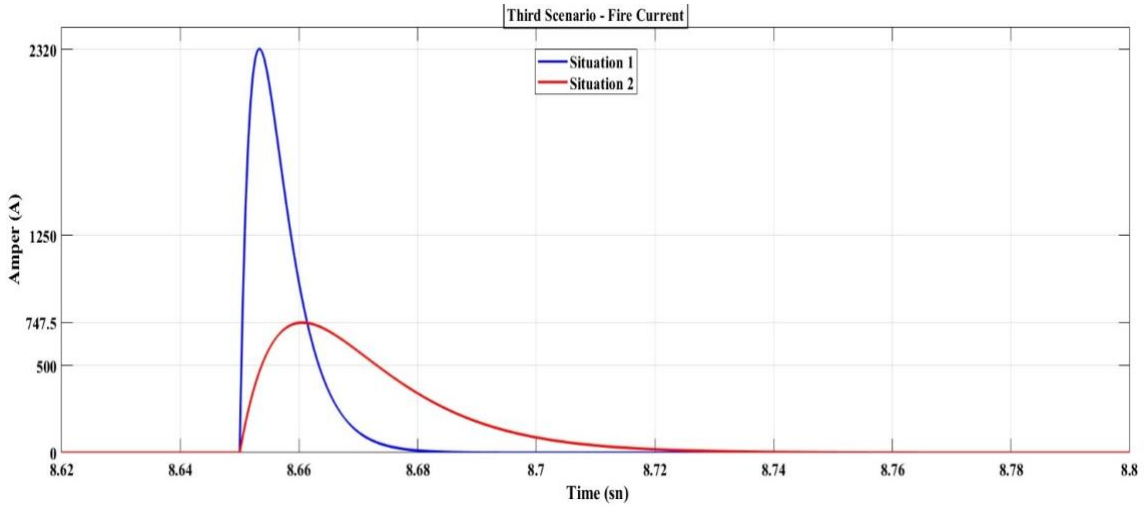

Figure 15. Scenario 3 – Firing Current Graph

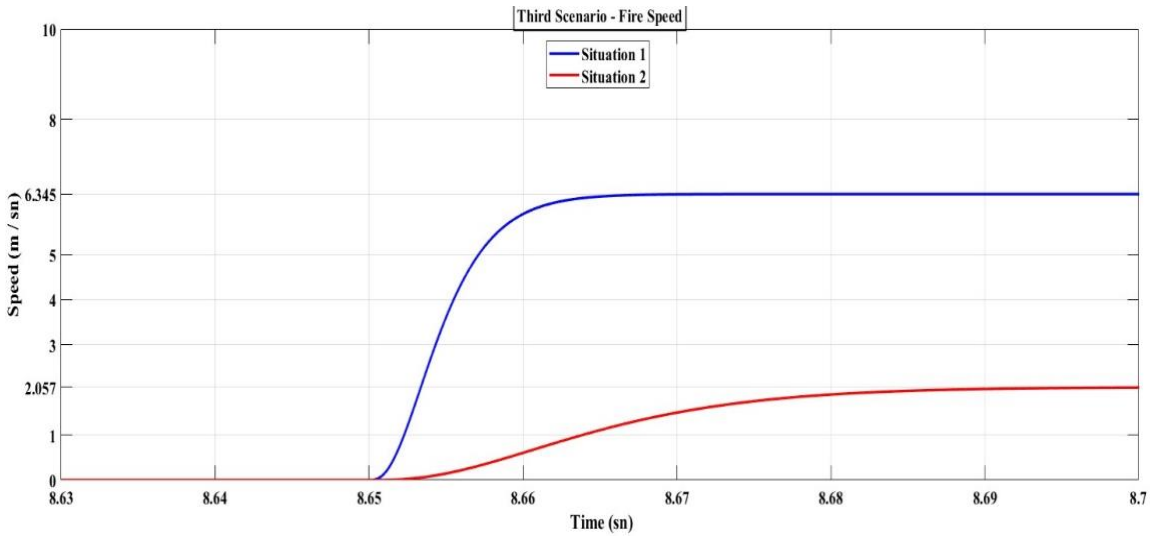

Figure 16. Scenario 3 – Firing Speed Graph

4.4. Fourth Scenario Results

In this scenario, the accuracy of the mathematical speed measurement model available in the literature on electromagnetic launcher systems is examined. In this context, depending on the same parameters, a comprehensive interpretation of the speed calculations of the mathematical speed measurement model in the literature will be presented. The current and speed graphs of the model created in MATLAB are shown in Figures 17 and 18, and the force, coil current and speed graphs of the model created in ANSYS Maxwell are shown in Figures 19, 20 and 21, respectively.

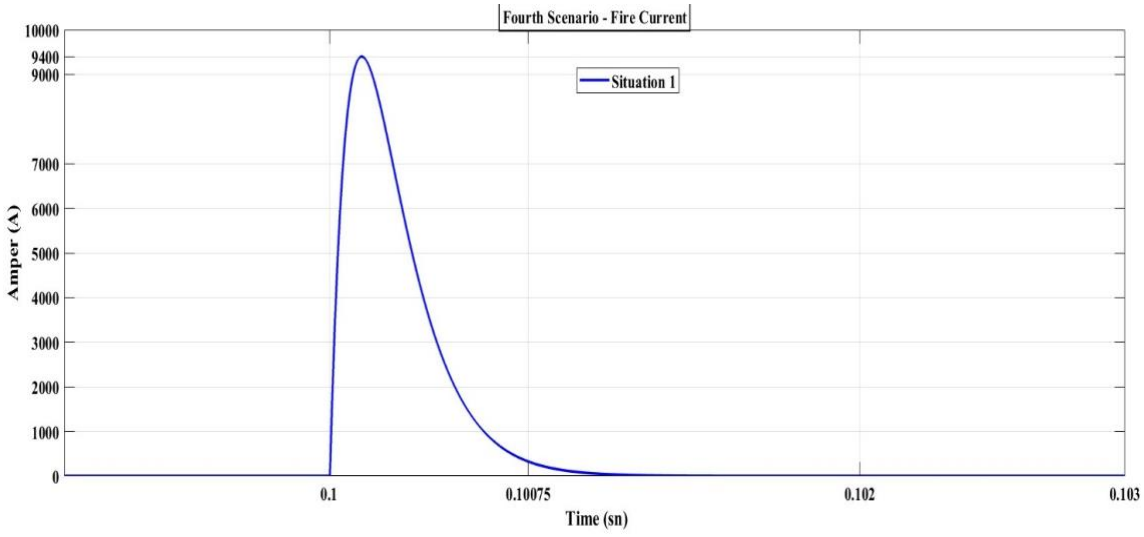

Figure 17. Scenario 4 – Firing Current Graph (MATLAB)

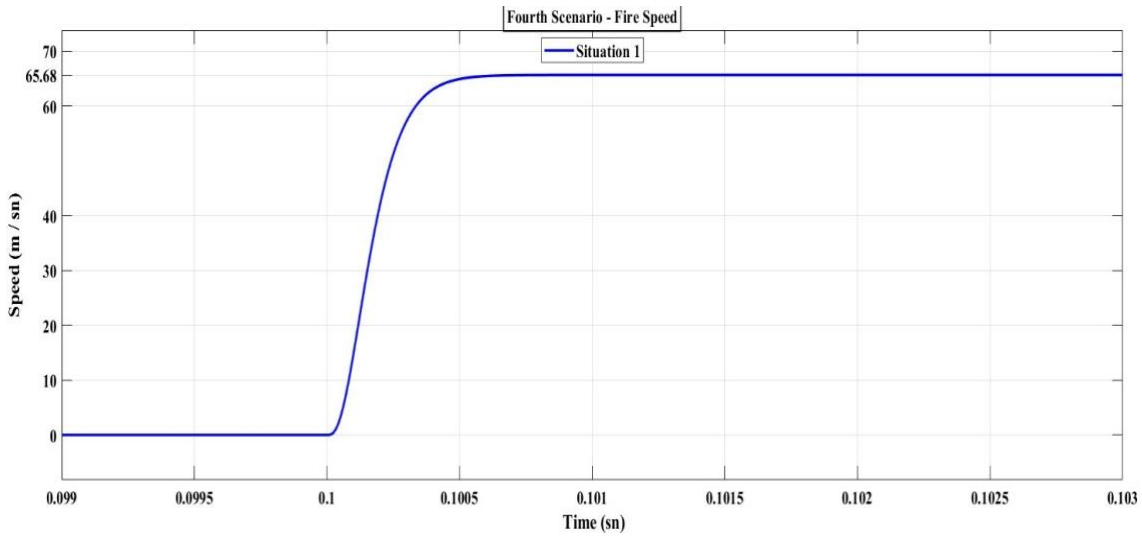

Figure 18. Scenario 4 – Firing Speed Graph (MATLAB)

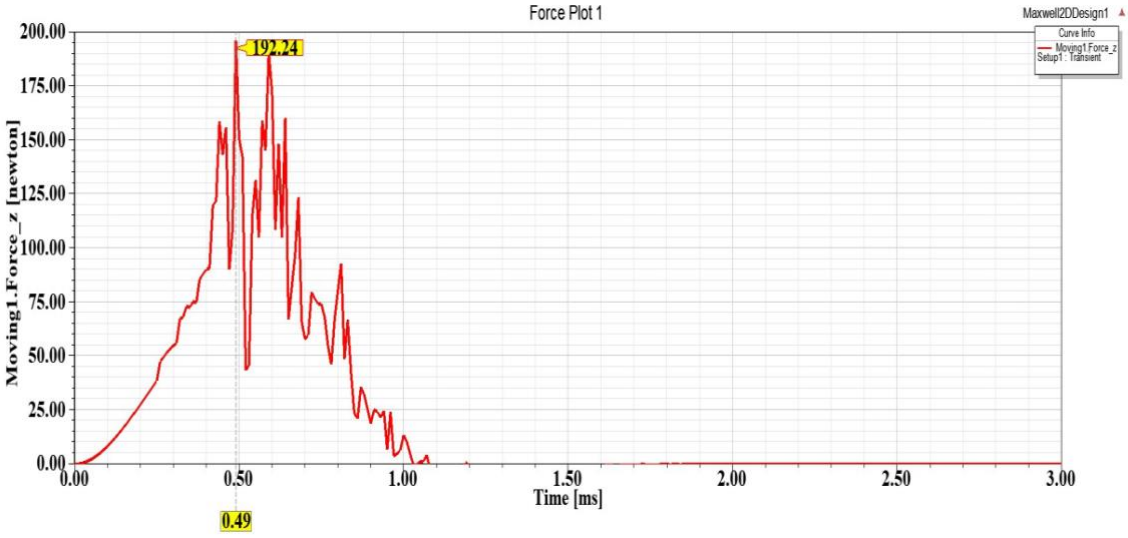

Figure 19. Scenario 4 – Firing Force Graph (ANSYS)

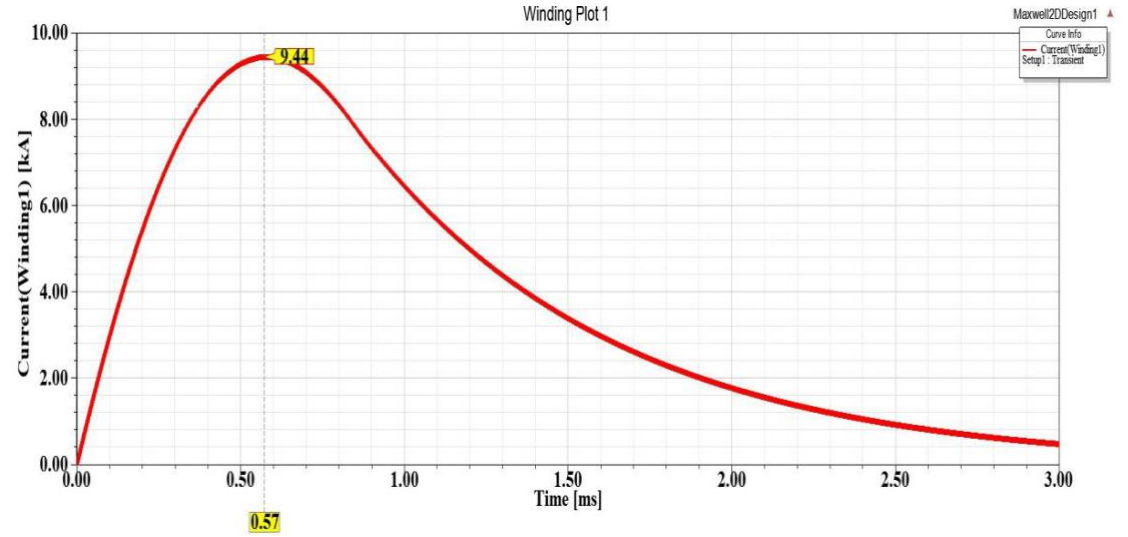

Figure 20. Scenario 4 – Firing Current Graph (ANSYS)

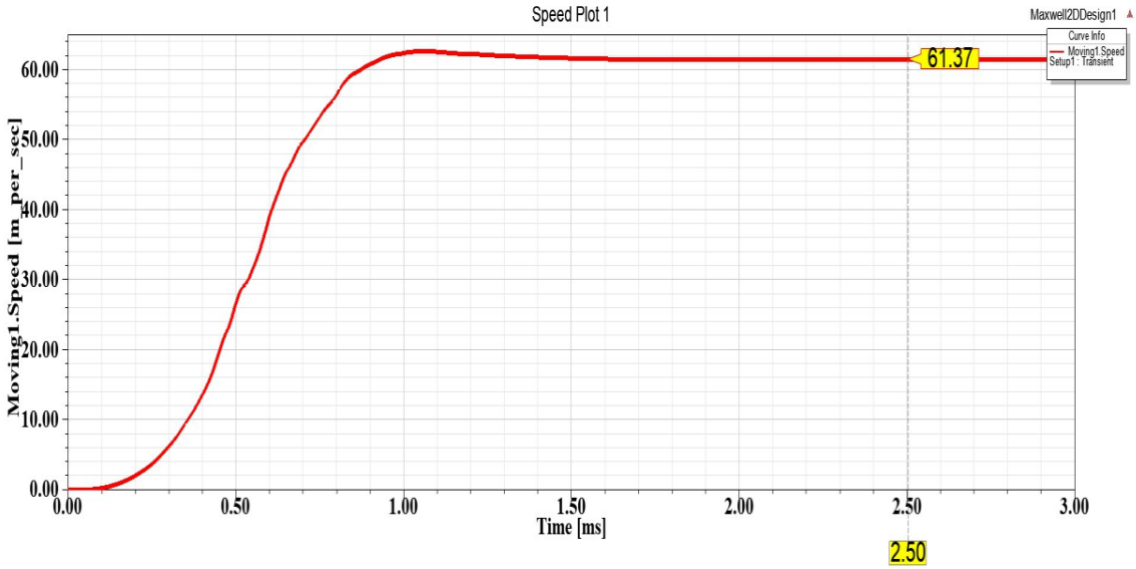

Figure 21. Scenario 4 – Firing Speed Graph (ANSYS)

In this scenario, differences in projectile speed were detected in simulation models performed in different programs with the same parameters. Since ANSYS provides a calculation process that includes electromagnetic field parameters as well as energy parameters, it is considered to be the most suitable program for the analysis of electromagnetic launcher systems.

When a comparative analysis was made between the mathematical velocity measurement found in the literature and the measurement using the finite element method including electromagnetic field parameters, a 7% difference in velocity was observed. In the speed measurement with ANSYS, there are projectile, barrel and air gap parameters and leakage flux values are included in the measurement. In this scenario, the effect of an air gap of 1 mm on the system is shown.

While the system efficiency was 14.379% in the test model made on MATLAB, the system efficiency was founded as 12.554% in the measurement model made on ANSYS. Compared to the speed measurement method obtained by using the ANSYS program, the measurement method in the literature has a margin of error of 7%. Based on the studies in the literature at different voltage levels, it was seen that this rate varied between 5% and 11% in two different test models.

4.5. Target and Human Detection Algorithm Results

This section shows the results of the target identification and detection models. Figure 22 shows the MATLAB / mfile output of the acoustic position model on the coordinate axis. In the figure, the squares at the origin represent the microphones, the + symbol represents the sound source defined in the theoretical model, and the red dot symbol represents the target resulting from the processing of the sound signal.

Based on the theoretical model, the experimental results show a deviation of 10% in the distance to the origin. The target angle deviated by 3.354 degrees with an increase of 6%. Table 7 shows the theoretical and experimental outputs of the positioning system. According to the output parameters, the fact that the sound encounter time differences of the microphones in the acoustic positioning system are close to each model shows that the linear algorithm using the time difference method can be used with the cross-correlation function with high accuracy.

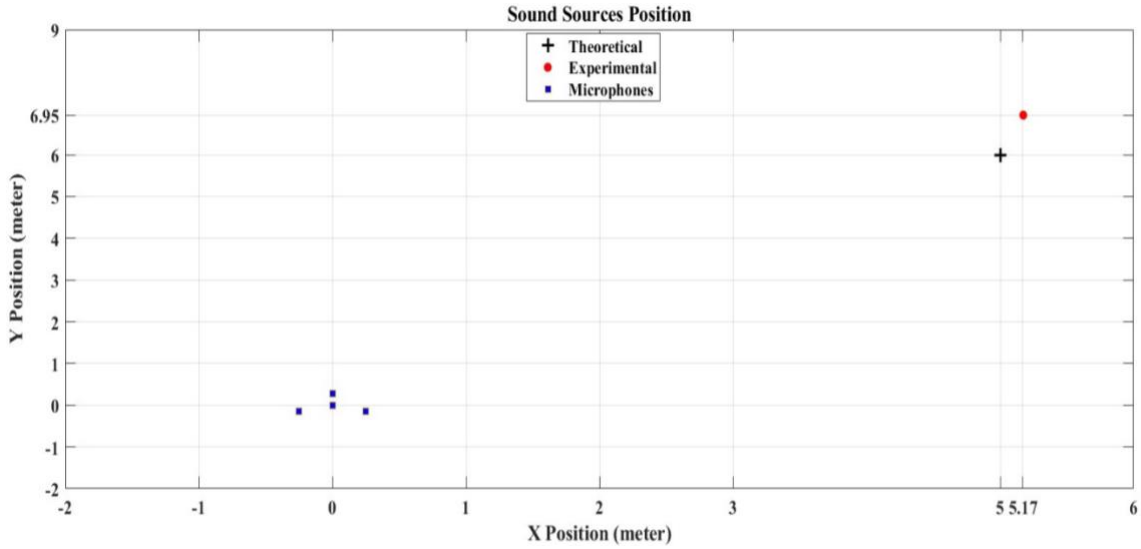

Figure 22. Output Results in Coordinate Axis

Table 7. Acoustic Positioning Parameters

Parameters	Theoretical Model	Experimental Model
Time Difference (ms)	[0.6352 0.126 -0.783]	[0.6431 0.080 -0.781]
Sample Value	0	48000
Signal Data Value	0	6600

Figure 23 shows the output results of the human detection system. In this system, when the input data of the object detector is set in a human-specific way, the number of people detected (M) value is 1 and the classification score [scores] value is 0.1997. These data are automatically transferred to Simulink and the switching is performed with these data. The reason why the scores value is far from 1 is that the image is blurred in the mfile before processing.

Figure 23. Human Detection System Result

5. Conclusions and Recommendations

Table 8 shows the results of scenarios 1, 2 and 3.

Tablo 8. Scenario Results

Parameters / Scenario	Scenario (1/2/3).1	Scenario 1.2	Efficiency Value (1)	Scenario 2.2	Efficiency Value (2)	Scenario 3.2	Efficiency Value (3)
Fire Current	2320 A	3820 A	+ % 2.2	4180 A	+ % 38.5	747.5 A	- % 1
Fire Voltage	145 V	238 V		85 V		145 V	
Fire Speed	6.345 m/sn	17.15 m/sn		65.63 m/sn		6.345 m/sn	

According to the velocity graph in Figure 11, it is observed that the projectile speed increases with increasing the voltage value of the capacitors. However, increasing the current consumption from the DC source for voltage gain will decrease the source voltage more rapidly. Additionally, increasing the voltage value will increase the electrical parameter values of the power electronics elements, thus increasing the system cost. Therefore, high voltage gain is not an effective method in portable DC-based systems.

In the second scenario, increasing the capacitance value by keeping the simulation time constant with the circuit parameters in the power stage of case 1 and case 2 was examined. According to the data obtained from Figures 14, when the capacitance value of the capacitor is increased, it is observed that the speed change is higher than in the first scenario when firing at the same charging time. It was

found that increasing the capacitance value was more effective than increasing the voltage value of the capacitors.

In this scenario, it can be seen that in low-power systems, the ability to fire at high speed with low voltages can be achieved. However, it is clearly understood that the charging time will be extended in order to provide sufficient damage power in portable systems. At this point, it is emphasized that power electronics play a critical role. Therefore, while increasing the capacitance value in portable systems has a positive effect on the damage level, it is not accepted as an effective solution method in terms of mission time.

When the situations in the third scenario are examined, it is observed that the speed value decreases in the shots performed by increasing the inductance value of the accelerator coil. In this case, the importance of keeping the inductance value of the coil as low as possible becomes apparent. However, in order to reduce the inductance value, it is necessary to reduce the winding diameter. At this point, the importance of winding technique is emphasized. For this reason, keeping the inductance value low in coil launchers may have a positive effect in terms of projectile speed; however, reducing the projectile size should not be considered as an effective solution method in terms of damage power.

In the last scenario, the parameters of the electromagnetic launcher system are kept constant and the results of two different simulation programs are compared. In the models and equations in the literature, the fact we do not consider the flux, which is the parameter of the force acting on the projectile during energy conversion, causes the projectile velocity to be calculated incorrectly. Although this speed difference is in single digits even in low power systems, it poses a risk in terms of system reliability. In the results obtained through ANSYS, since all components of the force acting on the projectile were calculated based on the electromagnetic field, the velocity changed with an accuracy of %7.

In the geometric and signal processing analysis of the target detection system, the amount of deviation in the position results is less than 10%, indicating that the algorithm has a high accuracy rate. The reason for this deviation is due to the numerical digit permission range of the source program that creates the audio recordings used in the simulation program.

Considering the results obtained, the way to be followed in the design of an electromagnetic launcher system is suggested as follows.

- First of all, the inductance value in the shooting model should be kept small to take into account the projectile size. For this purpose, winding technique or armature structure must be decided.

- Then the capacitance value must be determined. The equivalent capacitance value should be kept big enough not to adversely affect the charging time and system reliability. For this purpose, a load bank consisting of capacitor groups should be done instead of a single capacitor.
- In order to obtain the value of the current to be damped on the coil, the voltage value to be applied to the system and the power stage must be designed. It should be considered that the voltage value is inversely proportional to the charging time. Additionally, increasing the voltage level is not a preferred method since it increases the system cost and decreases its reliability.
- The capacitor and inductance values need to be selected to provide the damping period range specified in the literature. In the last stage, after determining the internal resistance value of the system, the damping resistance value should be selected.
- Since electromagnetic launcher systems consist of a charge and discharge cycle, switching signals must be associated with the mission. Therefore, it is essential that such systems are switched by sound or image.
- As demonstrated in the fourth scenario, leakage fluxes result in decreased system efficienency. Therefore, the magnetic materials to be used must be ferromagnetic. Reducing the leakage fluxes will greatly increase the system efficiency.

Authors' Contributions

All authors contributed equally to the study.

Statement of Conflicts of Interest

There is no conflict of interest between the authors.

Statement of Research and Publication Ethics

The author declares that this study complies with Research and Publication Ethics.

References

Abdo, M. M. M., El-Hussieny, H., Miyashita, T., & Ahmed, S. M. (2023). Design of A New Electromagnetic Launcher Based on the Magnetic Reluctance Control for the Propulsion of Aircraft-Mounted Microsatellites. *Applied System Innovation*, *6*(5), 81.

Akyazı, Ö., Bozdağ, M. O., & Akpınar, A. S. (2015). Elektromanyetik Fırlatıcılı Alan Savunma Sistemi Tasarımı ve Gerçeklenmesi. Fırat Üniversitesi Mühendislik Bilimleri Dergisi, 27(2), 43-50.

Akyazi, Ö. (2006). Elektromanyetik Fırlatıcılar (Yüksek Lisans Tezi). Karadeniz Teknik Üniversitesi, Fen Bilimleri Enstitüsü.

Baharvand, M., Kolagar, A. D., & Pahlavani, M. R. A. (2021). Design, Simulation, and Parameter Optimization of a MultiStage Induction Coilgun System. IEEE Transactions on Plasma Science, 49(7), 2256-2264.

Bresie, D. A., & Andrews, J. A. (1991). "Design of a reluctance accelerator." IEEE Transactions on Magnetics, 27(1), 623–627.

Çakır, O., Yazgan, A., Çakır, O., & Kaya, I. (2012). Farklı perspektiften zaman farkının varış ortalamasının alınması. In 2012 35. Uluslararası Telekomünikasyon ve Sinyal İşleme Konferansı (TSP) (s. 344-347). Prag, Çek Cumhuriyeti. https://doi.org/10.1109/TSP.2012.6256312.

Dalal, N., & Triggs, B. (2005). Histograms of Oriented Gradients for Human Detection. IEEE Computer Society Conference on Computer Vision and Pattern Recognition, 1, 886–893.

Dong, L., Li, S., Xie, H., Zhang, Q. ve Liu, J. (2018). Influence of Capacitor Parameters on Launch Performance of Multipole Field Reconnection Electromagnetic Launchers. IEEE Transactions on Plasma Science, 46(7), 2642-2646.

Ege, Y., Kabadayı, M., Kalender, O., Coramik, M., Citak, H., Yuruklu, E. ve Dalcali, A. (2016). A New Electromagnetic Helical Coilgun Launcher Design Based on LabVIEW. IEEE Transactions on Plasma Science, 44(7), 1208-1218.

Egeland, A. (1989). Birkeland' s Electromagnetic Gun: A Historical Review. IEEE Transactions on Plasma Science, 17(2), 73-82.

Fan, G., Wang, Y., Wang, P., Hu, Y. ve Yan, Z. (2020). Research on the Armature Structure Optimization of the Toroidal Reconnected Electromagnetic Launcher. IEEE Transactions on Plasma Science, 48(6), 2294-2300.

Fauchon, A., & Villeplee, L. O. (1920, January). Canons Electriques. Berger-Levrault.

İnger, E. (2013). Examination and Simulation of Electromagnetic Launch Systems. Doktora Tezi, Gazi Üniversitesi, Fen Bilimleri Enstitüsü, Ankara.

Jiang, P., Ergu, D., Liu, F., Cai, Y., & Ma, B. (2022). A Review of Yolo Algorithm Developments. Procedia Computer Science, 199, 1066-1073. https://doi.org/10.1016/j.procs.2022.01.135

Kaushik, Balakrishnan, Don, N., & Krish, A. (2005). A Review Of The Role Of Acoustic Sensors In The Modern Battlefield. 11th AIAA/CEAS Aeroacoustics Conference.

Kırıkcı, F. M. (2023). *Elektromanyetik Fırlatıcı Sistemlerin İrdelenmesi*. Yüksek Lisans Tezi, Karadeniz Teknik Üniversitesi, Fen Bilimleri Enstitüsü, Trabzon.

Liang, C., Xiang, H., Yuan, X., Qiao, Z. ve Lv, Q. A. (2021). Reverse Force Suppression Method of Reluctance Coil Launcher Based on Consumption Resistor. IEEE Access, 9, 62770-62778.

Lu, M., Zhang, J., Yi, X. ve Zhuang, Z. (2022). Advanced Mathematical Calculation Model of Single-Stage RCG. IEEE Transactions on Plasma Science, 50(4), 1026–1031.

McNab, I. R. (1999, January). Early electric gun research. IEEE Transactions on Magnetics, 35(1), 250-261. doi: 10.1109/20.738413.

Özuğur, Ö., & Leblebicioğlu, M. K. (2016). Akustik Algılayıcı Ağının Optimizasyonu ile Ateşli Silah Konumunun Tespit Edilmesi. Journal of Defense Sciences/Savunma Bilimleri Dergisi, 15(2).

Pages, C. G. (1845). New Electromagnetic Engine. American Journal of Science and Arts, 49, 131-135.

Praneeth, S. R. N., & Singh, B. (2022). Finite Element-Boundary Element Method Based Simulations of Electromagnetic Railgun in Augmented Configurations. IEEE Journal on Multiscale and Multiphysics Computational Techniques, 7, 320-327. doi: 10.1109/JMMCT.2022.3222529.

Sari, V. (2023). Effect of Change of Reluctance Launcher Parameters on Projectile Velocity. IEEE Access, 11, 90027-90037. https://doi.org/10.1109/ACCESS.2023.3307016.

Slade, G. W. (2005). A simple unified physical model for a reluctance accelerator. IEEE Transactions on Magnetics, 41(11), 4270–4276.

Su, X., Lin, F., Zhang, Q., Li, H., & Liu, Y. (2021). Optimal Design of a Multistage Induction Coil Launcher. IEEE Transactions on Plasma Science, 49(10), 3243-3250. https://doi.org/10.1109/TPS.2021.3113703.

Urruela, A., Sala, J., & Riba, J. (2006). Average Performance Analysis of Circular and Hyperbolic Geo Location. IEEE Transactions on Vehicular Technology, 55(1), 52–66.

Wan, X., Yang, S., Li, Y. ve Li, B. (2023). Inductance Gradient in Electromagnetic Launcher Under Channel Cooling Condition. IEEE Transactions on Plasma Science.

Wang, M., Cao, Y., Wang, C., Wang, H. ve Chen, J. (2016). Trigger Control Research of Electromagnetic Coil Launcher Based on Real-Time Velocity Measurement. IEEE Transactions on Plasma Science, 44(5), 885–888.

Zhao, J., Li, H., Zhao, B., Liu, J., Kong, L. ve Zhang, P. (2023). An Improved Pulsed Power Supply Circuit for Reluctance Electromagnetic Launcher Based on Bridge-Type Capacitor Circuit. IEEE Transactions on Plasma Science.